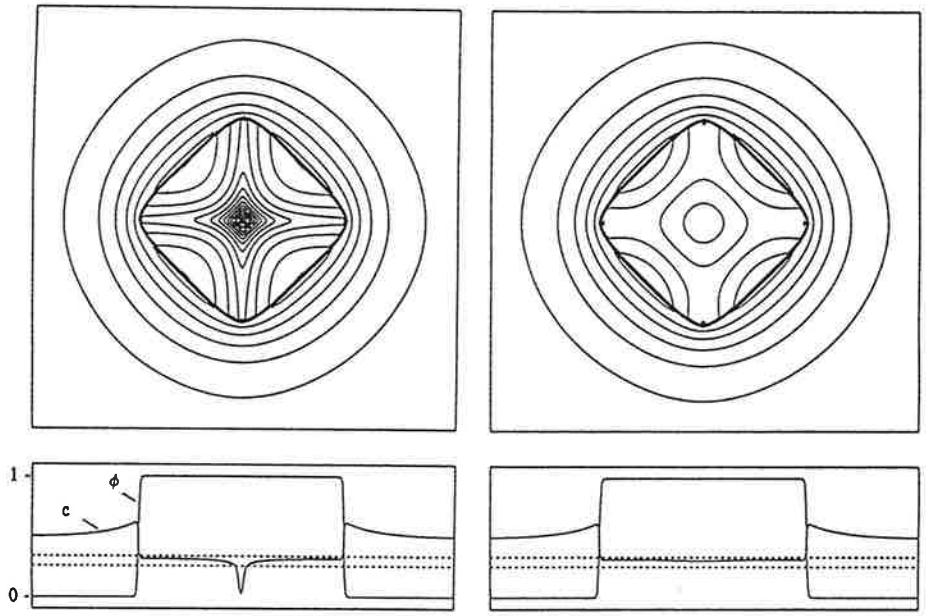

Figure 6 - Two dimensional simulation of isothermal growth from a pure A solid seed (c=0, ϕ=1) into a supersaturated binary alloy liquid with c=0.5. At the top are isoconcentrates in the liquid and solid. At the bottom are plots of ϕ and c along the horizontal centerline. Isoconcentrates are shown every 0.005 units for compositions between the dashed lines indicated at the bottom and otherwise every 0.025 units. The ratio of solid to liquid diffusion coefficients are 10^{-4} and 10^{-1} in (a) and (b) respectively. The anisotropy in ϵ was 5% and δ was set to 0.

References

1. J. S. Langer, in Directions in Condensed Matter Physics, edited by G. Grinstein and G. Mazenko, pp. 164-186, World Science Publishers, 1986.
2. B. I. Halperin, P. C. Hohenburg, and S. -K. Ma, Phys. Rev. B 10, 139 (1974).
3. J. B. Collins and H. Levine, Phys. Rev. B 31 6119 (1985).
4. G. Caginalp, Arch. Rat. Mech. Anal. 92, 205 (1986).
5. G. Caginalp, Phys. Rev. A 39 5887 (1989).
6. J. W. Cahn and J. E. Hilliard, J. Chem Phys. 28 258 (1958).
7. S. M. Allen and J. W. Cahn, Acta Met. 27 1085 (1979).
8. J. S. Langer and R. F. Sekerka, Acta Met. 23 1225 (1975).
9. R. Kobayashi, video tapes in Computational Optimal Geometries, edited by J. Taylor, Amer. Math. Soc., 1991.
10. R. Kobayashi, Bull. Jpn. Soc. Ind. Appl. Math. 1 22 (1991).
11. R. Kobayashi, to appear in Physica D (1992) and also in Physics of Pattern Formation in Complex Dissipative Systems, edited by S. Kai, World Science Publishers, (1992).
12. A. A Wheeler, W. J. Boettinger, and G. B. McFadden, Phys. Rev A, 45 7424 (1992).
13. A. A. Wheeler, W. J. Boettinger, and G. B. McFadden, submitted to Phys. Rev A.
14. O. Penrose and P. C. Fife, Phys. Rev. A43 44 (1990).
15. A. A. Wheeler, B. T. Murray, and R. J. Schaefer, submitted to Physica D.
16. M. J. Aziz, J. Appl. Phys. 53 1158 (1982).

MODELING OF UNDERCOOLING EFFECTS DURING THE DIRECTIONAL SOLIDIFICATION OF TURBINE BLADES

A. Ludwig, I. Steinbach*, N. Hofmann*,
M. Balliel*, M. van Woerkom*, P.R. Sahm

Foundry Institute
of the
Rhine-Westphalian Institute of Technology
FRG - 5100 Aachen

*ACCESS e.V.
FRG - 5100 Aachen

ABSTRACT

Undercooling in the "extremities" of turbine blade shrouds during directional and single crystal solidification leads to deteriorated properties. Thus it is desirable to reduce such effects by an appropriate process control. Based on the LKT-theory for dendritic growth into an undercooled melt and a simplified front tracking method a new numerical model is proposed which takes the undercooling ahead of the solidification front into account. The new algorithm is implemented into a finite element solver for modeling the single crystal directional solidification in Bridgman casting processes. The calculated temperature distribution within a turbine blade shroud is compared with the results of former equilibrium calculations.

INTRODUCTION

Numerical calculations of the temperature distribution within a 3D geometry, taking into account regions of undercooled melt is one of the important features of solidification modeling which is still rare in literature today (1,2). The reason for this fact is that in order to describe the propagation of the liquid/mushy interface into undercooled areas, the thermal and solutal conditions at the microscopic scale have to be known, together with macroscopic continuity equations. An exact solution of the growth part would require to consider a front tracking method at the scale of the entire process, but with a very complicated shape for the liquid/mushy interface. Since such a task is impossible with present computer power one has to apply appropriate simplifications.

Modeling of Casting, Welding and
Advanced Solidification Processes VI
Edited by T.S. Piwonka, V. Voller and L. Katgerman
The Minerals, Metals & Materials Society ©1993

Recently, M. Rappaz et al. have presented an algorithm which considers nucleation and undercooling effects during equiaxial solidification of binary alloys within 3D geometries (3,4). They assume that the thermal boundary layer is larger than the average grain size, leading to the consideration that the temperature within a grain is uniform. Applying a simplified nucleation model, they calculate cooling curves with recalescence and the corresponding grain size maps for materials with an equiaxed solidification structure.

In this paper a new model is presented which describes the propagation of a liquid/mushy interface into areas of undercooled melt by using a simplified front tracking method. It is based on the finite element solver CASTS for the 3D simulation of cast processes including a fully three dimensional net radiation calculation. The model is applied to calculate the undercooling and the accelerated growth within a turbine blade shroud which is undercooled during a conventional directional solidification process. In order to simplify the problem to the essential features a special dummy blade geometry is considered with two internal planes of symmetry (5).

MODEL DESCRIPTION

Considering a finite element mesh of a 3D geometry the nodes are, due to the actual aggregate state of the material, characterised as 'liquid', 'mushy' or 'solid'. In order to treat undercooling the liquid state must persist even when the temperature decreases below liquidus. In the presented algorithm there are two criteria for changing the state from 'liquid' to 'mushy':

i) the temperature of a mesh point decreases below a critical value (nucleation),

ii) a neighbouring mesh point already has the state 'mushy' and within the time step of the FEM calculation the advance of the envelope of the dendrite tips (liquid/mushy interface) reaches the considered mesh point (growth).

Further details about the second criterion are given below.

Whenever an undercooled mesh point changes its state from 'liquid' to 'mushy' its temperature is adjusted according to the requirement of heat balance:

$$T_i^n = T_L - (T_L - T_i^o)\frac{\rho c_p}{(\rho c_p)_{eff}} \qquad (1)$$

where T_L is the liquidus temperature and T_i^n, T_i^o are the new and the old temperature at mesh point i. $\rho\, c_p$ is the volumetric heat capacity of the melt (at T_L) and $(\rho\, c_p)_{eff}$ the so-called effective volumetric heat capacity (1), considering the latent heat of fusion.

After changing the status and adjusting the temperature according to equation (1) the finite element temperature solver calculates the temperature evolution for the next time step. As it is assumed that the solidification of the interdendritic melt takes place under equilibrium conditions, the temperature solver applies the equivalent specific heat method within the mushy region. The FEM temperature solver CASTS used for the calculation in this paper has been introduced in (2) and (6). During the temperature calculation no advance of the liquid/mushy interface is considered.

Following to the determination of a new temperature distribution a special subroutine describes the propagation of the dendrite tips. Thus, the growth process and the solution of the heat transport equation are decoupled.

In order to describe crystal growth into the undercooled melt on the macroscopic scale of the continuity equations the following straightforward technique has been applied:

All nodes which are in an undercooled state are entered into a list. This list is processed to estimate the mesh points where a change from liquid to mushy takes place.In order to decide whether a mesh point has to change its state, spherical shaped growth interfaces are considered to emerge from all neighbours which are in the 'mushy' or the 'solid' state as soon as the considered node starts to undercool. The growth rate v of this spherical growth is calculated applying the LKT-theory for dendritic growth into undercooled melt (7). The undercooling at the considered mesh point is used as bulk undercooling for the LKT-theory.

With this velocity the time of arrival at the considered node for each spherical interface is calculated by adding the time interval for the propagation (linear movement) to the time when the node starts to undercool. Comparison with the actual time used in the FEM calculation yields the decision whether a state change has to occur. The earliest arrival time is assigned to the considered mesh point as its time of change in state. Then the point is removed from the list of undercooled nodes and the state change is performed due to the upper description. If no interface arrives within the actual process time no change takes place. This procedure is performed on all undercooled nodes.

As it is possible that the solidification process traverses more than the actual FEM element in the given time step, it is necessary to repeat the above treatment on the list of mesh points if it is yet not empty and at least one state change occurred during the last processing,

If no further mesh point has to change its state the heat transport equation is solved for the next time step.

Similar to the LKT-theory which describes the dendritic growth into an undercooled melt of binary alloys the presented algorithm is also restricted to two-component systems. To apply the algorithm for the simulation of the directional solidification of superalloy turbine blades the multi-component superalloy is reduced to a quasi-binary alloy. On this score the diffusion coefficient D is estimated by applying the constitutional undercooling criterion:

$$D = \frac{\Delta T_0}{(G/v)_c} \qquad (2)$$

where ΔT_0 is the solidification interval and $(G/v)_c$ the critical G over v value for the appearance of the constitutional undercooling. G is the temperature gradient at the liquid/mushy interface. The distribution coefficient k is approximated as:

$$k = \frac{v_c}{v_t} \qquad (3)$$

where v_c and v_t are the critical velocities for the morphological transition planar-cellular and cellular-dendritic (8).

The values of $(G/v)_c$, v_c and v_t for the superalloy CMSX-6 are estimated by D. Ma et al. (9,10). The resulting D and k together with further physical properties of the superalloy CMSX-6 are listed in Table 1. The simulations in this paper were performed using this data.

Table 1 Physical properties of the superalloy CMSX-6 used in the calculations

liquidus temperature	T_L = 1340 ^{0}C
diffusion coefficient	D = 2.9 x 10^{-9} m^2/s
distribution coefficient	k = 0.31
solidification interval	ΔT_0 = 100 K
heat of fusion	L = 1.5 x 10^9 J/m^3
Gibbs-Thomson coefficient	Γ = 10^{-7} Km
heat capacity	ρc_p = 9.17 x 10^6 $J/(m^3 K)$
heat conductivity	λ = 30 W/Km

RESULTS AND DISCUSSION

With the algorithm presented above the directional solidification of a CMSX-6 superalloy dummy turbine blade within a Bridgman caster has been simulated using following process parameter set:

- upper graphite heater at 1450 ^{0}C,
- lower graphite heater at 1550 ^{0}C,
- a withdrawal speed of 1 cm/min is used after a steady state temperature distribution has been established,

- mean ceramic shell thickness of 10 mm,
- critical undercooling for nucleation set to 25 K.

For comparison, Fig. 1a shows a 3D graph of a turbine blade shroud for the time step where maximum undercooling appears calculated with the new algorithm and in Fig. 1b the corresponding situation determined under equilibrium conditions. For the sake of simplicity only one fourth of the whole blade is shown. Within the turbine shaft where directional growth takes place no significant difference occurs. Whereas in the outside region of the turbine blade shroud the difference due to the appearing undercooling is obvious.

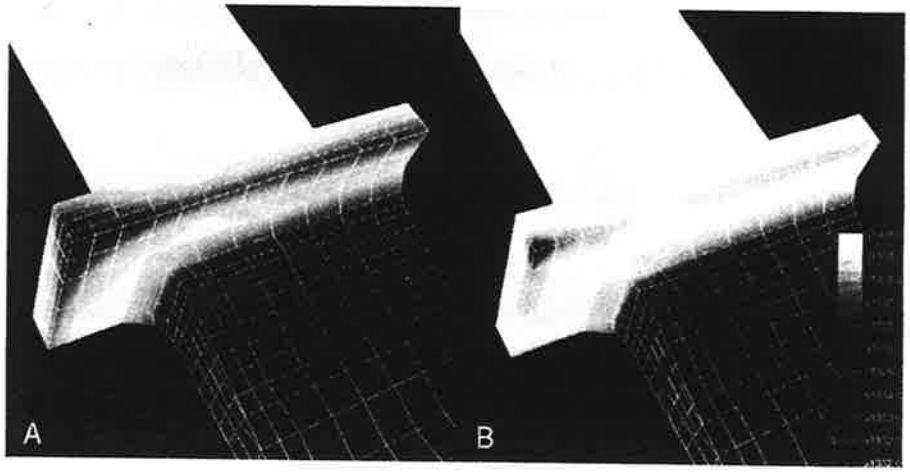

Figure 1 3D graph of a turbine blade shroud calculated with (a) and without (b) undercooling

Figure 2 shows a corresponding sequence of 3D graphs for different process times, where the rapid advance of the liquid/mushy interface into the undercooled region is illustrated. In Fig. 2a the shroud has reached the baffle region and thus starts to cool by heat radiation. Figure 2b and 2c reveal the temperature distribution just before and shortly after recalescence. It can be seen that an area of hot melt separates the undercooled region from the turbine shaft. As soon as the temperature of this hot area decreases below liquidus within only a small domain the liquid/mushy interface propagates very rapidly from the turbine shaft into the undercooled region. This is illustrated in Fig. 3 where the aggregate state of the turbine blade (a) and the time were the nodes change to ´mushy´ (b) is mapped just after recalescence occurs. The used time step during recalescence of about 0.2 s (the time step during the solidification of the shaft has been chosen to 2 s) was found to be too large to resolve the exact growth pattern.

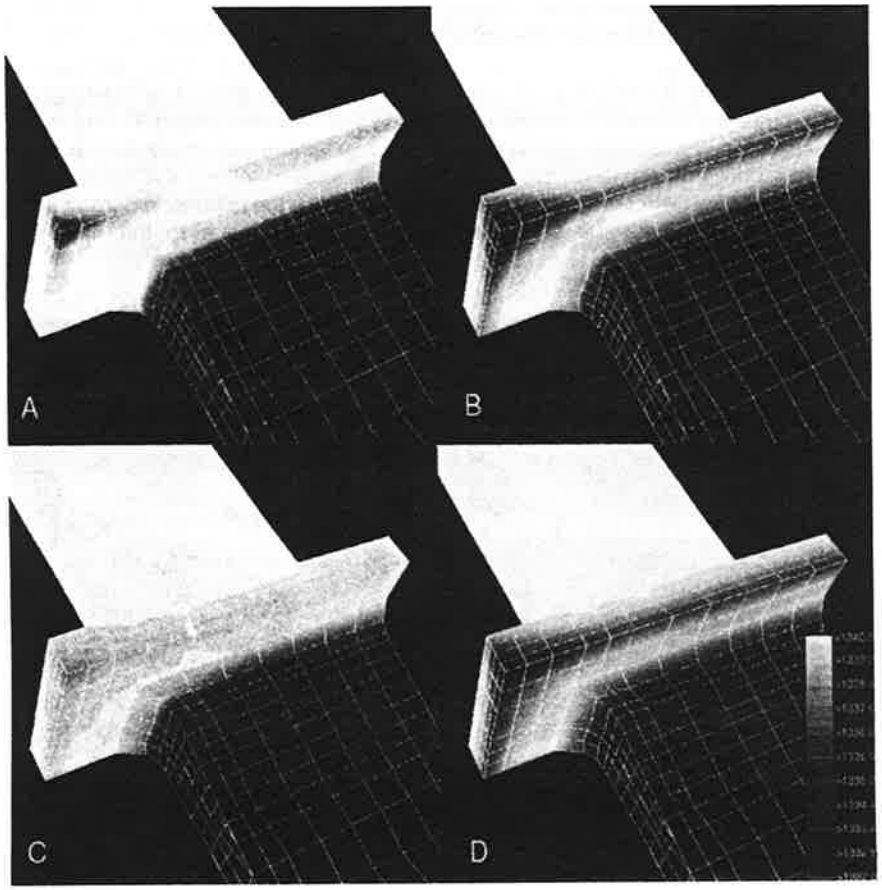

Figure 2 Sequence of 3D graphs according to different process times

In this calculation the maximum undercooling has been estimated to about 9 K. This is in good agreement with the experimental findings of U. Paul (11). He investigated the undercooling of the superalloy SRR99 within the shrouds of turbine blades experimentally.

In Fig. 4 different cooling curves determined at various locations within the shroud are shown. Curve 1 is calculated for the outer edge nearest to the baffle. Curves 2-5 are calculated at the same height but for different depths counted diagonally from this edge towards the turbine shaft.

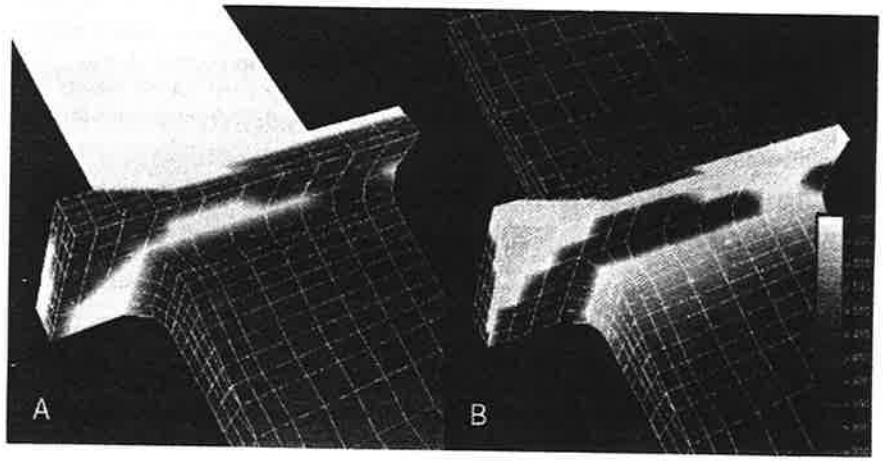

Figure 3 Aggregate state of the shroud just after recalescence (a) and time were the nodes change to 'mushy' (b). The dark nodes in (a) represents the 'mushy' and the bright ones the 'liquid' state.

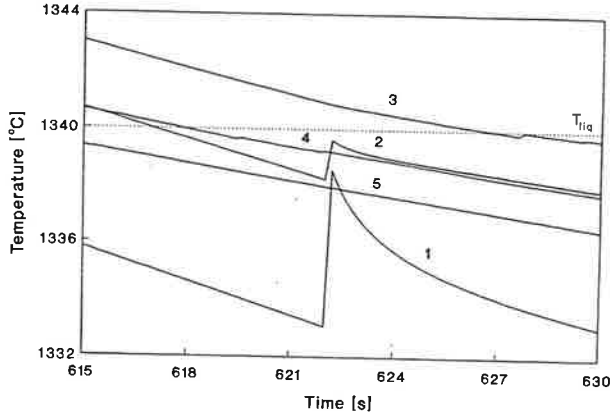

Figure 4 Calculated cooling curves at various locations within the shroud of the dummy blade

CONCLUSIONS

A new algorithm has been proposed to simulate the advance of a liquid/mushy interface into an undercooled melt on a macroscopic scale within a 3D geometry. This algorithm has been applied to simulate the undercooling within the extremities of turbine blade shrouds during the directional solidification within a Bridgman caster.

The simulation confirms that an undercooling of about 8 K appears at the extremities of the shroud. The solidification propagates from the turbine shaft very rapidly over a small area at the narrow side of the shroud into the undercooled areas. The corresponding recalescence takes less than 0.2 s. The new concept on which the presented algorithm is based on can be used not only for crystal growth into undercooled areas but also for directional growth situations.

ACKNOWLEDGEMENT

The authors would like to acknowledge to J. Spilker for valuable assistance in performing the changes in the code of the CASTS algorithm.

REFERENCES

1. M. Rappaz, Int. Mater. Reviews 34 (1989) 93
2. P.R. Sahm and P.N. Hansen, "Numerical Simulation and Modeling of Casting Processes for Foundry and Cast-House", International Committee of Technical Foundry Association CIATF, Zurich (1984)
3. J.L. Desbiolles, Ph. Thévoz, M. Rappaz, Proc. IVth Int. Conf. on Modeling of Casting and Welding Processes, Palm Coast (1988) 625
4. Ph. Thévoz, J.L. Desbiolles, M. Rappaz, Met. Trans. A 20 (1989) 311
5. F. Hediger and N. Hofmann, Proc. Vth Int. Conf. on Modeling of Casting, Welding and Advanced Solidification Processes, Davos (1991) 611
6. P.R. Sahm, W. Richter, F. Hediger, Gießereiforschung 35 (1983) 35
7. J. Lipton, W. Kurz, R. Trivedi, Acta Metall. 35 (1987) 957
8. W. Kurz and D.J. Fisher, Acta. Metall. 29 (1989) 11
9. D. Ma, "Solidification Behaviour of Ni-Based Superalloys", VDI-Verlag GmbH, Düsseldorf, Germany (1990)
10. D. Ma, R. Lentzen, P.R. Sahm, Gießereiforschung, 38 (1986) 106
11. U. Paul, "Single Crystal Dendritic Solidification of Turbine Blade Geometries ", VDI-Verlag GmbH, Düsseldorf, Germany (1992)

Microscopic Modeling of Microstructure Formation of A Nickel-Based Superalloy during Solidification and Verification

J. Zou[1], H. P. Wang[2], R. Doherty[1] and E. M. Perry[2]

[1] Department of Materials Engineering

Drexel University, Philadelphia, PA 19104

[2] GE Research and Development Center

Schenectady, NY 12301

ABSTRACT

The solidification behavior of a nickel based superalloy, its composition is similar to IN-738, has been determined by using a novel DTA technique which allowed us to measure the carbide, liquidus, solidus and eutectic temperatures on heating and the maximum undercooling and the local solidification time, on cooling, obtained in each sample. The concentrations of alloy elements at the center and edge of dendrite arms and in the carbide particles and matrix phase have been determined by WDS microprobe analysis, which helped us to identify the phases formed during solidification. The partitioning of each alloy element has been studied by the average ratio of concentration at the center of dendrite arm against that at the edge. The grain sizes and dendrite arm spacings at different cooling rates were measured on lightly etched sections of the samples which had been solidified in the novel DTA cooling runs while the eutectic size was measured on the polished section of the samples. An empirical relationship between the maximum undercooling and the grain size has allowed us to establish a quantitative nucleation law based on a previous analysis used in cast iron, steel, cast aluminum and aluminum aerospace alloys. A general solidification microstructure model initially developed for the binary system has been modified for a concentrated multi-component system such as iron and nickel based superalloys. This model predicts the microstructural parameters in the castings: grain size and its distribution, and the primary and secondary dendrite arm spacings, all as functions of cooling rate. The predictions of this model compare well with the measured results. This model should be applicable to other superalloys and intermetallics.

Modeling of Casting, Welding and
Advanced Solidification Processes VI
Edited by T.S. Piwonka, V. Voller and L. Katgerman
The Minerals, Metals & Materials Society ©1993